Thermochimica Acta, 212 (1992) 131–141
Elsevier Science Publishers B.V., Amsterdam

New directions in thermal analysis [1]

Bernhard Wunderlich [a,b]

[a] *Department of Chemistry, The University of Tennessee, Knoxville, TN 37996-1600 (USA)*
[b] *Division of Chemistry, Oak Ridge National Laboratory, Oak Ridge, TN 37831-6197 (USA)*

(Received 9 July 1991; accepted 30 March 1992)

Abstract

Thermal analysis has been stagnant for the last few years, perhaps with the exception of computer and software developments. Some of the more radically new ideas tested in our ATHAS laboratory are the following: (1) neural net routines for the extrapolation of heat capacities beyond the limits of measurements and for the inversion of heat capacities into approximate vibrational spectra; (2) single-run heat capacity instrumentation using double difference measurements; (3) the analysis for mesophases and rigid amorphous fractions in polymeric materials which are of importance for high-tech composites; (4) the complete molecular dynamics simulation of the motion in polymer crystals to such a precision that heat capacities, and later possibly also heats of transition, can be derived. The discussed "new directions" indicate that much can be done to enhance the quantitative aspects of DSC so that thermal analysis will certainly become even more important in the 21st century.

THE DEVELOPMENT OF THERMAL ANALYSIS

The roots of our advanced thermal analysis system (ATHAS) as sketched in Fig. 1 go back to the 1950s, to the beginning of continuous differential calorimetry supported by electronic control and heat-loss recording, as carried out in Professor M. Dole's laboratory [1]. In the next 10 years, major developments led to what is now known as differential scanning calorimetry (DSC) or, more precisely, as scanning isoperibol twin-calorimetry [2]. Its beginning can be traced to small-mass continuous differential calorimetry, first described by Professor F.H. Müller in 1960 [3], followed by the production of a commercial instrument based on electronically controlled heat flow, known as the Perkin-Elmer DSC [4]. The schematic diagram of the measuring principle of the Perkin-Elmer DSC is illustrated in Fig. 2. Parallel to this evolution from elaborate, discontinuous, adiabatic

Correspondence to: B. Wunderlich, Department of Chemistry, The University of Tennessee, Knoxville, TN 37996-1600, USA.

[1] Presented at the 20th Annual NATAS Conference, Minneapolis, MN, 20–26 September 1991.

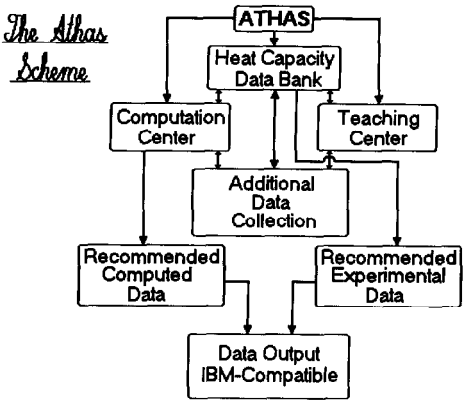

Fig. 1. Linkage between the various parts of the ATHAS.

calorimetry using large masses of sample for high precision, to small, convenient, automatically recording differential scanning calorimeters requiring only 1–100 mg of sample, was the improvement of differential thermal analysis (DTA) to precision calorimetry. This technique had its beginning at the turn of the century (for an extensive list of early publications in DTA, see ref. 5). Initially DTA was rather qualitative in the measurement of heat (but not in temperature, where classical, in-the-sample thermocouple placement will outdo any calorimeter). Its schematic is shown in Fig. 3. In the 1960s the difference in the precision of measurement of heat between calorimetry and DTA became a matter of debate, mainly through the introduction of the DuPont DSC (now TA Instruments) which also made extensive use of electronic controls.

The question as to when to call an instrument a DTA or a DSC is largely academic. The ICTA definition that "thermal analysis is the measurement of changes in physical properties of a substance as a function of temperature whilst the substance is subjected to a controlled temperature program" makes thermal analysis the global expression, also including, among many

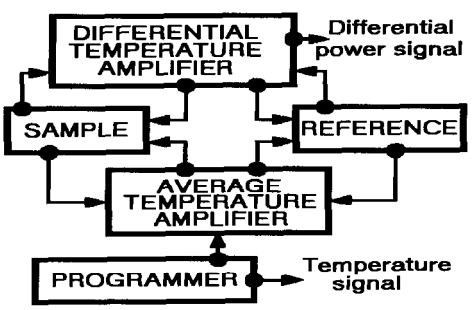

Fig. 2. Diagram of the Perkin-Elmer DSC [2].

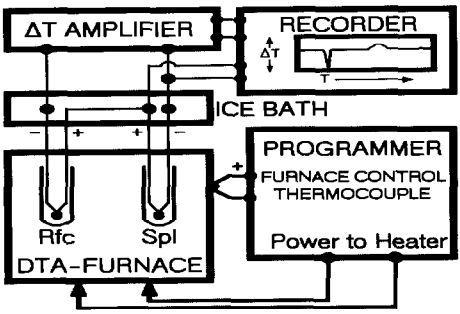

Fig. 3. Schematic of a DTA [2].

other techniques, calorimetry. Calorimetry, in contrast, has been narrowly defined for many years. It is a technique that is used to measure heat. If the result of an experiment is thus given in joules, calorimetry has been performed (and if the experiment is done in a scanning mode in a differential set-up, it is DSC), i.e. every DSC is DTA, but naturally not all DTA is DSC.

A further advance took place with the introduction of computer technology, starting in the 1980s. The ATHAS laboratory was among the first to make use of this technique [6]. In retrospect, one must say that the increasingly sophisticated computers have not brought about a major advance in precision or ease of operation. Our early measurements of heat capacity on 100% crystalline polyethylene with a Perkin-Elmer DSC 1 [7] compare favorably with those on poly(amino acid)s using the latest DSC 7 [8]. Even the volume of quality calorimetric data described in the literature has not increased significantly in the last 10 years, and learning how to use a DSC with computer control is by no means easier than without. A further problem had already been pointed out at the 8th ICTA in Bratislava [9]: "It is important to produce hardware which can be combined with any type of software". Because the commercially offered combined instrument and software packages are usually proprietary, they are not conducive to improvement by the user. In fact, a recent application for funds from our laboratory to NIH was denied because, among other reasons, an unpublished software program was thought by the reviewer to be proposed for heat capacity computation. The enormous effort that went into the development of the software seems also to have stifled further advance in hardware. Perhaps there will now be progress because software development is slowing down and several new companies have entered into the DSC market.

A series of new directions of thermal analysis that have been tested in our ATHAS laboratory and that seem to promise to advance calorimetry into the 21st century, are outlined below.

NEURAL NET ROUTINES

A neural network is a computational system made up of a number of simple, yet highly connected layered processing elements called nodes or neurons, which processes information by its dynamic response to external information as outlined in Fig. 4 (see for example ref. 10). These networks were originally biologically inspired to perform in a manner analogous to the basic functions of neurons. The initial performance of such networks was rather poor, but by now a second generation of software is available that seems to open the field to a wide range of applications in thermal analysis.

The network is specified by its architecture, transfer functions, and learning laws. It typically learns in a computation-intensive step by establishing weights that, when applied to the inputs of the nodes, will yield the required output. In an initial test, it could be shown, for example, that once the network has learned the general shape of heat capacity as a function of temperature, it can extrapolate with good precision to low temperatures where measurement is difficult. For training, the network was taught a series of computed heat capacities from 100 to 300 K in steps of 10 K, using the ATHAS. This led to weights being adjusted so that the heat capacities from 10 to 90 K were properly predicted. For new inputs, the heat capacities at low temperature could be predicted to better than $\pm 1\%$ as shown in Table 1 [11]. Note that the typical experimental precision is $\pm 1\%$.

A second computation involved the neural-network inversion of the Tarasov function used for the parameterization of the skeletal heat capacity [12]. The inversion of the heat capacity into the two frequency parameters Θ_3 and Θ_1 could be shown to be by far faster and better averaged than

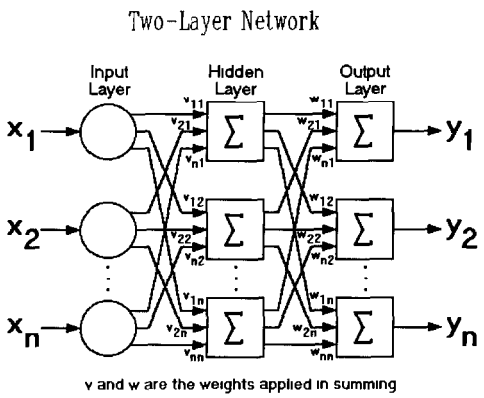

Fig. 4. Schematic of a typical neural network.

TABLE 1

Heat capacity data predicted by neural networks

Polymer	Predicted value	Measured value	Percentage error	Temperature (K)
PEN	5.1826	5.1987	−0.31	10
	19.7206	19.8736	−0.77	20
	32.5057	32.7414	−0.72	30
	43.1375	43.3324	−0.45	40
	52.8020	52.8549	−0.10	50
	62.1784	62.0543	+0.20	60
	71.5633	71.2073	+0.50	70
	80.9630	80.4163	+0.68	80
	90.3907	89.7000	−0.78	90
	99.7745	99.0121	+0.77	100
PE	0.0995	0.1002	−0.67	10
	0.7411	0.7440	−0.39	20
	1.9143	1.9230	−0.45	30
	3.2316	3.2475	−0.49	40
	4.5225	4.5434	−0.46	50
	5.7424	5.7695	−0.47	60
	6.8786	6.9083	−0.43	70
	7.9231	7.9597	−0.46	80
	8.8866	8.9190	−0.35	90
	9.7150	9.7835	−0.70	100
PVF	0.5279	0.5276	+0.06	10
	3.0382	3.0285	+0.32	20
	6.1560	6.1321	+0.39	30
	9.1264	9.0964	+0.35	40
	11.9300	11.8967	+0.28	50
	14.6152	14.5889	+0.18	60
	17.1803	17.1631	+0.10	70
	19.6439	19.6380	+0.03	80
	21.9969	21.9947	+0.01	90
	24.1685	24.2024	−0.14	100
PS	1.1263	1.1236	+0.24	10
	6.7264	6.7009	+0.38	20
	13.9038	13.8760	+0.20	30
	20.5449	20.5593	−0.07	40
	26.3592	26.4491	−0.34	50
	31.4193	31.5740	−0.49	60
	35.8665	36.0756	−0.58	70
	39.8522	40.0928	−0.60	80
	43.6114	43.8746	−0.60	90
	47.1929	47.4062	−0.45	100

Key: PEN, poly(ethylene-2,6-naphthylene dicarboxylate); PE, polyethylene; PVF, poly(vinyl fluoride); PS, polystyrene.

TABLE 2

Neural network predictions

Predicted values (K) by the neural network [a]		Input C_v computed or from experimental data	
Θ_1	Θ_3	Θ_1	Θ_3
450.4	148.6	450	150
529.7	191.0	530	190
489.4	108.5	490	110
518.8	156.9	519 ± 10 [b]	158 ± 2 [b]

[a] C_v generated from the Tarasov equation with Θ_1 and Θ_3 given in columns 3 and 4 except for the last row, which was generated from the experimental C_v of polyethylene.

[b] Polyethylene, experimental data, Θ_1 and Θ_3 previously estimated using trial inversions to fit the experimental heat capacities.

the present system of trial inversions at each temperature, as is illustrated in Table 2.

Because only the learning step of the network takes a considerable amount of computer time, it is possible to have the learning done on a supercomputer and to transfer the once-established weights to a PC for everyday use. One may also speculate that it may be possible to have the network learn the contents of a whole data bank, such as the ATHAS data bank of heat capacities of macromolecules, and to predict unknown heat capacities by making use of the collective knowledge gained over the years in many laboratories.

SINGLE-RUN HEAT CAPACITY

Perhaps one of the reasons why little quantitative calorimetric information results from the large number of existing thermal analyzers is that it takes three runs to establish a heat capacity baseline [2]. In recent years we were able to predict [3] and finally to show that by using double-differential scanning calorimetry with the triple cell of TA Instruments [14,15] one can measure heat capacity in a single run. Figure 5 gives a schematic and lists the basic equations of the calorimeter. The required software has been developed [16] and is at present in the process of being refined, to be available to interested users through the ATHAS system [17]. This new method of thermal analysis joins the prior instrumental developments of ATHAS that included fast DDTA with up to 10000 K min^{-1} heating or cooling rates [18], pressure DTA, of up to 15 MPa gas pressure or 300 MPa hydraulic pressure [19], and the early computerization of DSC [6].

MESOPHASES AND RIGID AMORPHOUS FRACTIONS

Calorimetry and study of the data bank of thermal properties have led to a series of discoveries. Comparing many samples it became obvious that

Single Run DSC Based on the TA 912 Cell

$$C_{pB} = C_{pA}(\Delta T_B/\Delta T_A) \quad \text{First approximation}$$

$$C_{pB} = C_{pA}\frac{\Delta T_B(1 + d\Delta T_B/dT_B)}{\Delta T_A(1 + d\Delta T_A/dT_A)} \quad \text{Second approximation}$$

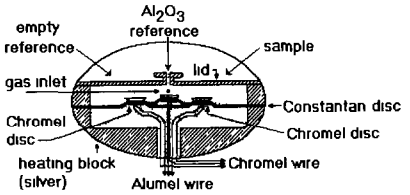

Fig. 5. Single-run DSC [13–16].

there are three major types of mesophase, and not, as thought before, only two [20]. The new phase is that of conformationally disordered crystals (condis crystals). Figure 6 illustrates the position of the new mesophase relative to the "classical" phases and the other mesophases, as well as the corresponding glasses. Per mole of disordered bonds of a molecule, 9–12 J K^{-1} mol^{-1} entropy increase can be observed. This rule permits the interpretation of DSC traces that show multiple-phase behaviour. Typical examples of condis crystals are polyethylene, polytetrafluoroethylene, and *trans*-1,4-polybutadiene. More than 100 condis crystals have been identified in a major review [21] and give the basis of an expansion in the range of applications for quantitative thermal analysis.

While the fusion in one or several steps is an endothermic transition with an increase in disorder (entropy), glasses will undergo the solid–liquid transition at the glass transition temperature. Studying the increase in heat capacity at the glass transition, it was found that it is a materials constant

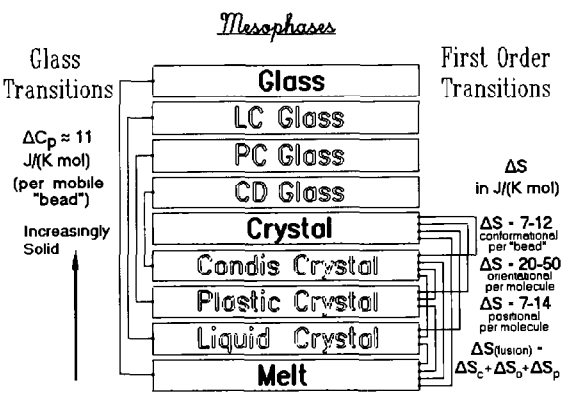

Fig. 6. Schematic of the possible types of condensed phases [20,25].

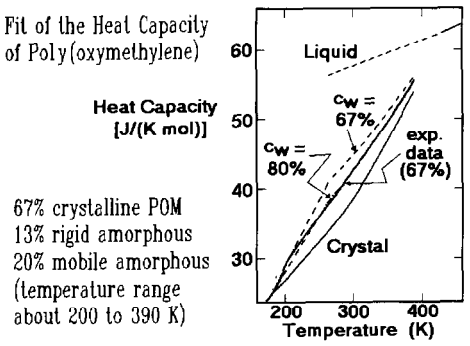

Fig. 7. Evaluation of the rigid amorphous fraction in poly(oxymethylene) [23].

of about 11 J K^{-1} mol^{-1} for each mole of mobile part in the molecule (bead) [22]. Applying this concept to semicrystalline polymers revealed that some of the amorphous glass, most likely the part closely attached to the crystal surface, may not become mobile at the observed glass transition temperature. The measured change in heat capacity at the glass transition is less than that expected in a fully amorphous sample reduced by the fraction of crystallinity. This deficit was ascribed to a rigid amorphous fraction [23]. Figure 7 shows the evaluation of the rigid amorphous fraction by matching of heat capacities for poly(oxymethylene).

The rigid amorphous fraction has been shown to be prominent in many of the more rigid macromolecules such as PEEK [24], poly[oxy-1,4-(2,6-xylylene)] [25] and poly(phenylene oxide) [26]. Figure 8 reproduces the data for poly(thio-1,4-phenylene). The faster the crystallization (lower crystallization temperatures), the larger the rigid amorphous fraction. Its influence on the physical properties of the polymer is that of a crystal, i.e. it increases the modulus, while its influence on the annealing behavior is opposite to that of a crystal, i.e. it decreases in amount on annealing.

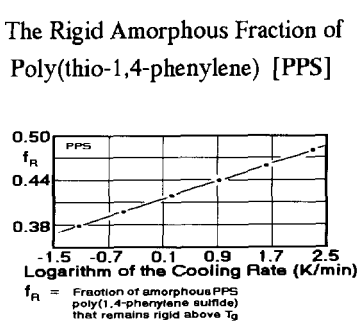

Fig. 8. The rigid amorphous fraction of polyphenylene sulfide as evaluated by Cheng et al. [26].

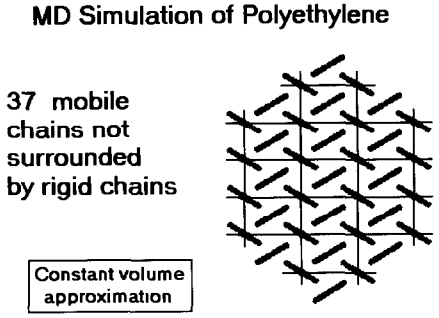

Fig. 9. Crystal segment for simulation by molecular dynamics: view down the crystallographic c axis (a is horizontal, b is vertical), total of 3700 CH_2 groups [29].

These two new areas of thermal analysis should result in an increase in the volume and value of thermal analyses applied to the evaluation of materials. In many cases thermal analysis is able to decide quickly between the various types of mesophase, and for many samples the rigid amorphous fraction can at present only be quantitatively identified by thermal analysis.

MOLECULAR DYNAMICS SIMULATION

Another recent advance that relates to thermal analysis is the full molecular dynamics simulation of crystals. Crystals with up to 10 000 atoms have been analyzed in our laboratory in this fashion for times of up to 100 ps. Figure 9 illustrates a typical crystal segment for the computer simulation. Each line represents a segment of 100 CH_2 sequences viewed down the crystallographic c axis (z direction), i.e. looking down the zig-zag plane, with CH_2 groups being placed alternately at the ends of the lines. In the molecular dynamics simulation, classical mechanics calculations are used to study the simultaneous motion of all atoms of the crystal for a given length of time, starting from well-defined initial conditions [27]. At any moment the kinetic energy of the crystal gives information about the temperature:

$$KE = \frac{3}{2}NkT = \sum_{i=1}^{100m} \frac{p_{x_i}^2 + p_{y_i}^2 + p_{z_i}^2}{2M}$$

Because the total energy of the initial state is set, the temperature difference between two simulations can be used to calculate the heat capacity. In this way full linkage between the actual atomic motion and the macroscopic thermal analysis can be established. For polyethylene a 30-year-old puzzle of high heat capacity before melting could be resolved as resulting from conformational defect generation [28]. The defects are clearly shown in Fig. 10 in a time sequence of projections of the lower third of seven inner

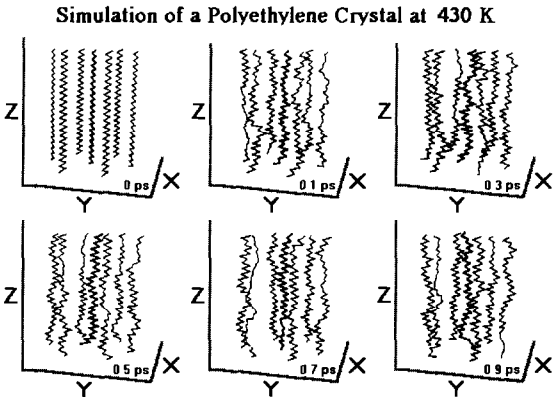

Fig. 10. Polyethylene crystal simulation from 0 to 0.9 ps at 430 K (1 ps $= 10^{-12}$ s). The directions x, y, z are parallel to the crystallographic a, b, c directions [29].

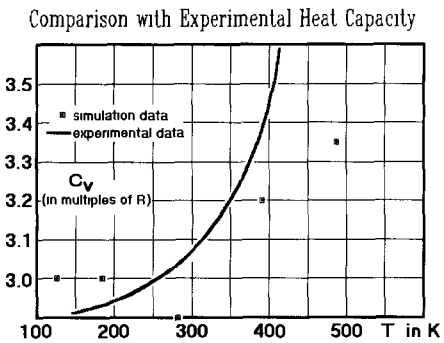

Fig. 11. Excess heat capacity of polyethylene caused by defects as shown in Fig. 10: curve, experimental data; points, simulation of a crystal as in Fig. 9 (inner chain data only) [29].

chains of the polymer crystal at 430 K. Figure 11 shows the qualitative fit between the measured and simulated heat capacities of the crystal drawn in Fig. 9. A detailed study of the influence of crystal parameters, temperature and crystal size has presented the possibility of linkage of thermal analysis, molecular motion and mechanical properties [29].

ACKNOWLEDGMENTS

This work was supported by the Division of Materials Research of the National Science Foundation, Polymers Program, Grant no. DMR 8818412, and the Division of Materials Science, Office of Basic Energy Sciences of the U.S. Department of Energy, under Contract DE-AC05-84OR21400 with Martin Marietta Energy Systems, Inc.

REFERENCES

1 B. Wunderlich and M. Dole, J. Polym. Sci., 24 (1957) 201.
2 B. Wunderlich, Thermal Analysis, Academic Press, Boston, MA, 1990.
3 F.H. Müller, G. Adam and H. Martin, Kolloid Z., 172 (1960) 97; 193 (1963) 1, 29.
4 E.S. Watson, M.J. O'Neill, J. Justin and N. Brenner, Anal. Chem., 36 (1964) 1233; US Patent 3,263,484.
5 W.J. Smothers and Y. Chiang, Handbook of Differential Thermal Analysis, Chemical Publishing, New York, 1966.
6 U. Gaur, A. Mehta and B. Wunderlich, Therm. Anal., 13 (1978) 71.
7 B. Wunderlich, J. Phys. Chem., 69 (1965) 2078.
8 K. Roles and B. Wunderlich, Biopolymers, 31 (1991) 477.
9 B. Wunderlich and P. Fellner, Thermochim. Acta, 110 (1987) 67 (quote of remark by E. Gmelin, p. 69).
10 P.D. Wasserman, Neural Computing, Van Nostrand Reinhold, New York, 1989.
11 J.A. Darsey, D.W. Noid, B. Wunderlich and L. Tsoukalas, Makromol. Chem. Rapid Commun., 12 (1991) 325.
12 D.W. Noid, M. Varma-Nair, B. Wunderlich and J.A. Darsey, J. Thermal Anal., in press.
13 B. Wunderlich, J. Therm. Anal., 32 (1987) 1949.
14 Y. Jin and B. Wunderlich, J. Therm. Anal., 36 (1990) 765.
15 Y. Jin and B. Wunderlich, J. Therm. Anal., 36 (1990) 1519.
16 Y. Jin and B. Wunderlich, to be published (1992).
17 Write to the author for a biannual report, the heat capacity data bank or information on specific techniques or polymers.
18 B. Wunderlich and D.M. Bodily, J. Polym. Sci., Part C, 6 (1964) 137.
Z.Q. Wu, V.L. Dann, S.Z.D. Cheng and B. Wunderlich, J. Therm. Anal., 34 (1988) 105.
19 B. Wunderlich and R.C. Bopp, in H.G. Wiedemann (Ed.), Proc. 3rd ICTA, Thermal Analysis, Vol. 1, Birkhauser Verlag, Basel, 1972, p. 295.
20 B. Wunderlich and J. Grebowicz, Adv. Polym. Sci., 60/61 (1984) 1.
21 B. Wunderlich, M. Möller, J. Grebowicz and H. Baur, Conformational Motion and Disorder in Low and High Molecular Mass Crystals, Adv. Polym. Sci., Vol. 87, Springer-Verlag, Berlin, 1988.
22 B. Wunderlich, J. Phys. Chem., 64 (1960) 1052.
23 H. Suzuki, J. Grebowicz and B. Wunderlich, Br. Polym. J., 17 (1985) 1.
24 S.Z.D. Cheng, M.-Y. Cao and B. Wunderlich, Macromolecules, 19 (1986) 1868.
25 S.Z.D. Cheng and B. Wunderlich, Macromolecules, 20 (1987) 1630.
26 S.Z.D. Cheng, Z.Q. Wu and B. Wunderlich, Macromolecules, 20 (1987) 2801.
27 D.W. Noid, B.G. Sumpter, B. Wunderlich and G.A. Pfeffer, J. Comput. Chem., 11 (1990) 236.
28 D.W. Noid, B.G. Sumpter and B. Wunderlich, Makromol. Chem. Rapid Commun., 10 (1989) 377.
29 B.G. Sumpter, D.W. Noid and B. Wunderlich, J. Chem. Phys., 93 (1990) 6875.